

Robust Motion Estimation Improves Underwater Sonar Accuracy

Lian Yu¹, Nicola Neretti², Nathan Intrator²

¹Department of Mathematics, Beijing Normal University, 19 Xijiekouwai St., Beijing 100875, P.R.China

²Institute of Brain and Neural Systems, Brown University, Box 1843, Providence, RI 02906, USA.

Abstract – Underwater sonar system is currently the best solution to distinguish a hazardous target from the harmless objects or a flock of fish at a far distance in the water, subsequently protect the harbors' security. A good sonar system should have the ability to surveille a long range, in the meantime reserve a high accuracy. Noise is a crucial problem effecting the accuracy. One possible solution to increase the signal-to-noise ratio (SNR) is to average return signals over multiple sonar pings. A problem with this approach is the relative motion between the sonar and the target during pinging which strongly reduces the effect of the averaging. In this paper, we present a robust motion estimation using multiple receive sensors that estimates the relative motion between multiple pings and aligns all the pings to a base ping through appropriate motion compensation. We further show that the fusion of multiple pings for time-delay estimation after realignment has the potential of improving both the resilience to noise and the accuracy, consequently increasing the operating range.

Keywords – Underwater sonar, motion estimation, noise, robust.

I. INTRODUCTION

Protecting military harbors requires good ability to “see” underwater. In particular, it requires the ability to distinguish between floating objects, divers, unmanned vehicles and living ocean creatures from a flock of fish to whales. Underwater sonar is currently the best solution to this task. It works through transmitting sonar pings and receiving echoes from targets from which a representation of the environment is created. For a multi-aperture sonar system, using beamforming or image reconstruction technic, a 2-D underwater image can be obtained. Clearly, a good system, should detect threats at a sufficient distance to enable time for proper response, thus challenging underwater sonar to increase its range without sacrificing its accuracy. High accuracy can improve recognition and detection sensitivity as well as reduce false alarms. Sonar accuracy is strongly dependent on the background noise. In fact, when the noise level is above a certain threshold, accuracy falls rapidly [1]. One possible solution to this is to average returns over multiple sonar pings. Such averaging is likely to reduce the effect of the noise by a factor of $1/\sqrt{n}$, n is the number of successive sonar pings. A problem with this approach is the relative motion between the sonar and the target during pinging which strongly reduces the effect of the averaging. As the range of the sonar is affected by the sensitivity to background noise, improving on this sensitivity will increase the sonar range. While sending n pings requires n times the energy level of a single ping, there are several reasons why

sending a high peak energy is less desirable than sending n times a lower energy signal. This has to do with the properties of the sound transducer, as well as security issues attempting to stay undetected.

Although there are six (three translational and three rotational) possible motion variables, only two have significant effect on the multi-receiver array. They are the sway (the horizontal shift from the mean position of the array) and the yaw (the horizontal angular rotation around the center of the array). There are three options to determine the motion errors: using hardware systems to record the different degrees of freedom of the sonar system; using motion estimation algorithms based on the raw data and using the information from the reconstructed image of the raw data. Presently available navigation instruments, such as inertial units, are either expensive or unable to provide adequate level of accuracy [2]. Currently, most algorithms using the raw sonar returns are based on correlation or phase estimation. The correlation algorithms include amplitude-only envelope correlation, complex baseband signal correlation [3] and the shear average [4] method. The performance of the phase estimation technique relies heavily on the choice of the phase estimation kernels. A detailed comparison of the different phase estimation kernels was given in [5]. The most popular used phase estimate technique is the ‘displaced phase centre’ (DPC) algorithm [6], also known as the ‘redundant phase centre’ (RPC) algorithm [7]. The RPC algorithm uses the phase and time shifts in the cross-correlation of the positions of the collocated phase centres to interpret the displacements of the receiver array. The image based motion estimation algorithms use 2-D cross-correlation on the reconstructed images to estimate yaw and sway. In [8], a “beam to beam correlation” technique was described in which a 2-D cross-correlation of the adjacent ping images was used to estimate the relative yaw angle. A “displaced ping imaging autofocus” (DPIA) algorithm was introduced in [9], in which a 2-D cross-correlation on the Fourier domain of the low-accuracy images was done to estimate the yaw. In [10], a high-order correlation (HOC) scheme was developed for postprocessing the beamformed images in order to significantly minimizing the incident of false detections. Generally the raw data based motion estimate algorithms simply average the estimation result of multiple elements, so they can only estimate sway and suitable for higher signal-to-noise ratio (SNR) situation. On the other hand, the image based approaches use the full information of multiple elements, so they are more tolerant to lower SNR. But they depend on a basic assumption that one

or several dominant targets should appear in the interesting area. This assumption limits the usefulness of the image based approaches to detect more complicate structure objects.

In this paper, we introduce a robust motion estimation technique which improves the effect of averaging of multiple pings. We concentrate the current paper on estimating sway and yaw of the relative motion between sonar and target. We demonstrate both the improved accuracy and improved resiliency to noise that can be obtained by the proposed motion estimation method.

II. METHODOLOGY

A. Motion Model

The proposed sonar accuracy enhancement is based on averaging multiple echo returns obtained from multiple sonar pings. Such averaging can effectively increase accuracy if the relative motion of the sonar and target are compensated. After motion compensation, the pings will be aligned, to give an effective stationary relation between the sonar and the target. We estimate the relative motion between the first ping and all the other pings so as to align the sonar to the location during the first ping.

Similar assumptions as in [9] hold: 1) The medium is stable during pinging (i.e. there is good temporal correlation between pings) so any time shifts in the cross-correlation of the positions of the sensors can be interpreted as specific displacements of the receiver sensor array. 2) The ‘stop and hop’ scenario where the sonar is assumed to be stationary during the period between transmitting at a particular position and receiving all of the echoes before moving to the next transmitting position. 3) Since all the sensors are mounted on a straight steel cable, the sensors move as a rigid body. It is to say, the sensors move as a line and the displacements of the sensors between any two pings are also on a line. As we assume that the target range is much larger than the sway and the yaw, the differences of the time delays of the echoes between two pings for all sensors are approximately on a straight line.

The sway and yaw motion between two pings are modeled in Fig. 1. The sonar system model so it now has one transmitting sensor and N receiving sensors where each sensor has an integer index $n \in [1, N]$ and the index of the middle sensor (overlaid with transmitting sensor) is m which is either $N/2$ or $(N+1)/2$. The sensors are equally separated by distance d . The displacement ΔX of sensor m is the sway between two pings. The angle θ_{yaw} of ping 2 with ping 1 is the yaw angle (we assume that the sensors of the first ping i.e. sensors of ping 1 in Fig. 1 are all aligned in the direction perpendicular to the ping direction). If ΔX and θ_{yaw} can be estimated correctly, then through shift and tilt motion compensation, ping 2 can be aligned to ping 1. This is implemented by adding a certain time delay to the received signal of the relevant sensor of ping 2 and aligning each

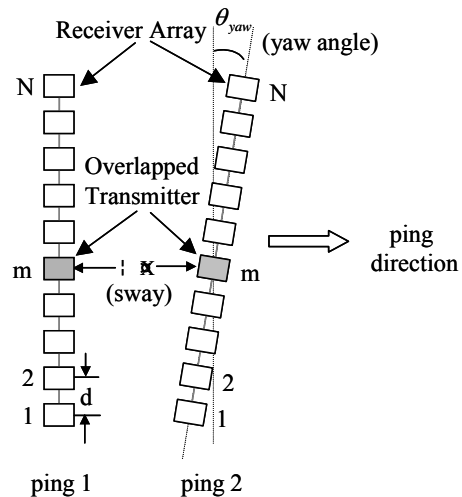


Fig. 1. Modeling motion between two pings.

sensor’s signal of ping 2 to the corresponding sensor’s signal of ping 1. Due to noise, the estimated displacements of the sensors are not exactly on a straight line, but are distributed around some certain line. Therefore some kind of line fitting method should be used to estimate the line. We have found that the least square line fitting (LSLF) method for estimating the line properties is not sufficiently robust in our case. This is due to the outliers in the displacement estimation that will be observed when noise level is higher. We propose a more robust line fitting method that is based on the mode of the distribution - an improved mode line fitting (IMLF) method. Thus, the sway and yaw are estimated respectively by the center and the angle of the line.

For multiple pings, we set the first ping as the baseline. The relative motion between each ping to the first ping is estimated and each ping is aligned to the first one by correcting the relative motion. The aligned multiple pings are then used for an averaged time-delay estimation or multiple pings fusion time-delay estimation. As the motion between the pings is corrected, the accuracy of the sonar is greatly improved with the increasing of the number of pings.

B. Motion Estimation

The motion estimation approach is based on the raw data from one transmit sensor and multiple receive sensors. Here we consider any two pings. The displacement of each receive sensor depends on the sway and yaw between the two pings. Thus by following the process summarized in the flow diagram of Fig. 2, the actual sway and yaw required to align the two pings into coincidence can be estimated simultaneously. We denote the received raw echo data from sensor n of two pings as $e_{1,n}(t), e_{2,n}(t)$ respective to ping 1 and ping 2, where t is the delay time. The received echo is passed through a matched filter for cross correlation with the

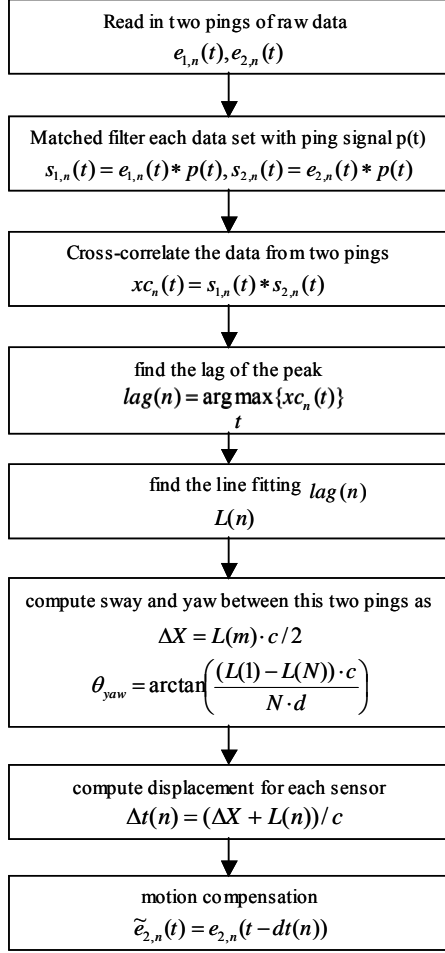


Fig. 2. Flow diagram for estimation and compensation of sway and yaw between two pings

pinging signal

$$\begin{aligned} s_{1,n}(t) &= e_{1,n}(t) * p(t) \\ s_{2,n}(t) &= e_{2,n}(t) * p(t) \end{aligned} \quad (1)$$

where $p(t)$ is the ping signal and $*$ defines cross-correlation in t . The output of the matched filter from two pings of the same sensor is cross-correlated to yield:

$$x_{c,n}(t) = s_{1,n}(t) * s_{2,n}(t) \quad (2)$$

where n is the index of the sensor. The lag of the peak of the cross-correlation result is expressed as

$$lag(n) = \arg \max_t \{x_{c,n}(t)\} \quad (3)$$

which is the temporal displacement between two pings for sensor n . The displacement data for all sensors is collected. A set of points consists of

$P = \{(1, lag(1)), (2, lag(2)), \dots, (N, lag(N))\}$, where $1, 2, \dots, N$ is the index of the sensors (as the intervals of the sensors are equal, we can always use their index to substitute their real distance). Using suitable line fitting method (which

we will introduce in the following section), we seek a line that is the linear fitting curve of the set P . We denote the value of the line at index n by $L(n)$, which is the estimated displacement of sensor n , for $n = 1, 2, \dots, N$. The sway and yaw angle between two pings is computed as follow

$$\Delta X = L(m) \cdot c / 2 \quad (4)$$

$$\theta_{yaw} = \arctan \left(\frac{(L(1) - L(N)) \cdot c}{N \cdot d} \right) \quad (5)$$

where ΔX is the sway and θ_{yaw} is the yaw angle, m is the index of the middle sensor, c is the speed of sound, d is the space between adjacent receiving sensors. Because the received data is a two-way echo, transmit from transmitting sensor to the target and return from the target to the receiving sensor, the time delay of the received echo between two pings for each sensor due to the displacement of the pings can be calculated by

$$\Delta t(n) = (\Delta X + L(n)) / c \quad (6)$$

where $\Delta t(n)$ is the time delay of the received echo data between two pings for sensor n , ΔX is the displacement of the transmitting sensor, $L(n)$ is the displacement of the receiving sensor n . The motion compensation for each sensor received data of ping 2 is

$$\tilde{e}_{2,n}(t) = e_{2,n}(t - \Delta t(n)) \quad (7)$$

where $\tilde{e}_{2,n}(t)$ is the motion corrected data for sensor n of ping 2. After motion compensation implemented to each sensor's received echo data, ping 2 will be aligned to ping 1. The two pings are independent, so the scheme adapts to any pair of pings. Especially, for a set of multiple pings, using the scheme, all the pings will align to the first ping. The aligned multiple pings can be treated coherently. As the motion between the pings is corrected, the accuracy of the sonar or the resolution of the reconstructed image in a noise environment will be greatly improved with the increasing of the number of pings.

C. Least Square Line Fitting (LSLF)

A popular line fitting method is the least square line fitting. In this part we prove that the middle of the least square fitting line segment of a set of points is equal to the mean point of the set of points. Suppose there are a set of points $(x_i, y_i), i = 1, 2, \dots, n$, the linear fitting curve through the points using least square method is

$$\tilde{y} = ax + b \quad (8)$$

$$\text{where, } a = \frac{(\frac{1}{n} \sum_{i=1}^n x_i y_i) - (\frac{1}{n} \sum_{i=1}^n x_i)(\frac{1}{n} \sum_{i=1}^n y_i)}{(\frac{1}{n} \sum_{i=1}^n x_i^2) - (\frac{1}{n} \sum_{i=1}^n x_i)^2} = \frac{\overline{xy} - \bar{x}\bar{y}}{\overline{x^2} - (\bar{x})^2}$$

$$b = (\frac{1}{n} \sum_{i=1}^n y_i) - a(\frac{1}{n} \sum_{i=1}^n x_i) = \bar{y} - a\bar{x}$$

for each point, the fitting point will be

$$\tilde{y}_i = ax_i + b \quad (9)$$

Let the middle point of the fitting line segment is (x_m, y_m) which can be expressed as

$$x_m = \left(\frac{1}{n} \sum_{i=1}^n x_i \right) = \bar{x} \quad (10)$$

$$y_m = \left(\frac{1}{n} \sum_{i=1}^n \tilde{y}_i \right) = \left(\frac{1}{n} \sum_{i=1}^n (ax_i + b) \right) \quad (11)$$

$$= a \left(\frac{1}{n} \sum_{i=1}^n x_i \right) + b = a\bar{x} + b = \bar{y}$$

This is to say that the middle point of the least square fitting line segment of a set of points is equal to the mean point of the set of points. Given a set of displacements for two pings' sensors immersed in noise, using least square line fitting (LSLF) method to search the fitting line of the displacements and using the middle of the fitting line as the estimated sway of the sensors is equivalent to using the mean of the displacements to estimate the sway. It is proved in [11] that the mean of the distribution is not contributing at all to the resilience to noise.

D. Improved Mode Line Fitting (IMLF)

In [11], it is argued that a more robust statistics method for estimating time-delay, such as the median, can improve the resiliency to noise as the number of pings increases. Best results are obtained by using the mode of distribution of the estimates from the multiple pings. In our case, using multiple pings is equivalent to using multiple sensors as the sensors lie on a straight line. The time delay estimation from multiple pings is equivalent to the sway estimation from multiple sensors' displacement. However, the mode can not be used directly. In the noise free case, although the displacements of the sensors are positioned on a straight line (a rigid moving of sensor array), the line can be tilted due to the yaw. In a noisy case, the displacements will be distributed around a tilted straight line with some possible outliers (Fig. 3). When the distribution of the echo displacements between any two pings is analyzed along a line that is parallel to the tilted sensor array, the observed distribution has minimal variance and the mode is a good estimator of the center of the displacements. In the tilt angle distribution case, we divide the range into intervals with the same width. Each interval forms a bin. In the simplest case, we define the mode by the bin which

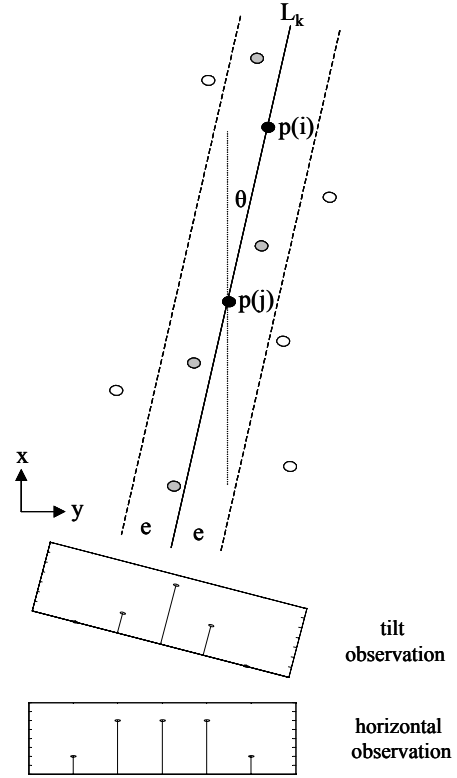


Fig. 3. The sketch of the improved mode line fitting method. Black points $p(i)$ and $p(j)$ are the selected pair of points. Solid line L_k is the fitting line through $p(i)$ and $p(j)$. The gap between two dashed line is the bin of L_k . The width of the bin is $2e$. θ is the tilt degree between line L_k and x-direction. Gray points are the points inside the bin. Circle points are the points outside the bin. The histogram of the points distribution in the range is shown at the bottom for tilt angle distribution and straight angle distribution respectively.

contains the largest number of points. A line through the mode with the tilt degree of the distribution can be the fitting line for the displacements. We introduce an improved mode line fitting (IMLF) algorithm to search the fitting line.

Let suppose there is a set of points named from 1 to N . Only the lines which through at least two points are selected (the tilt degree of the line is limited to some certain degree). For such a line, we compute the bin centered at the line and having a certain width. The number of points contained by the bin is counted. The fitting line of the points is the line which contains the largest number of points in its bin.

The steps of the algorithm are

step 0: Input a set of points $p(i) = (x(i), y(i)), i = 1 \dots N$, N is the number of points, select an engaged gap e as the width of the bin which is centered around a selected line, select a degree θ_{\max} as the maximum tilt degree of a suitable line, set $k = 1$

step 1: Select a pair of points

$$\{p(i), p(j)\}, i, j = 1, \dots, N, i \neq j$$

step 2: Compute the line l through the point pair $\{p(i), p(j)\}$

step 3: Calculate the tilt degree θ between line l and x direction
if $abs(\theta) > \theta_{max}$, then throw line l , go to step 1
else reserve line l and put l in the suitable line set as L_k , continue step 4

step 4: Search the points whose distance to line L_k is less than ϵ , save the number of these points as $num(k), k = k + 1$

step 5: Iterate step 1-4 for all the point pairs

step 6: Search the line L_k which contains the maximum number of points as $K = \arg \max_k \{num(k)\}$

step 7: Output line L_K as the fitting line of the point set d

The sketch of this algorithm is shown in Fig. 2.

III. RESULTS

The following describes simulation results obtained with the Filed2 sonar simulator [12]. We used one transmitter and 10 receivers linear array. The pinging signal was a Mexican hat at a center frequency of 300kHz with a bandwidth of 20kHz and a 6.7 μs duration. Both the ping signal and its auto-correlation had a sharp peak and two symmetric negative part with lower magnitude. The target was a point reflector surrounded by scatterers. For each ping, we added a random motion (sway and yaw) to the ping. The motion was relative to the first ping. The sway was uniformly distributed random displacement in $[-2\lambda, 2\lambda]$, where λ is the wave length of the pinging signal. The yaw was uniformly distributed random degree between $[-2^\circ, 2^\circ]$. White Gaussian noise was added to each sensors' received signal. The SNR is measured by the peak-signal-to-noise-RMS (power). We estimated the motion of the ping using LSLF and IMLF methods. The estimated sway and yaw were compared to the actual sway and yaw and the errors were recorded. For multiple pings, the root mean square error was calculated as a function of the SNR. Fig. 4 and 5 depict the sway and yaw estimation error (RMSE) (m) vs. SNR. In Fig. 4, the sway estimation errors using LSLF (cross curve), median (triangle curve) and IMLF (circle curve) methods respectively are shown. It indicates that the best sway estimation is obtained by the proposed IMLF method. The IMLF has the smallest estimation error when the SNR higher than 0db and also has the smallest breakpoint at 3db as the breakpoint of the median method and LSLF are at 4db and 7db respectively. The RMSE of all the three methods is over the std of the active sway at -2db. It means that the motion estimator will not obtain the correct estimation if the SNR is lower than -2db. Fig. 5 depicts the yaw estimation errors by using LSLF (cross curve) and IMLF (triangle curve) estimation respectively. It shows that the IMLF is better than LSLF. The breakpoint of IMLF is 2db

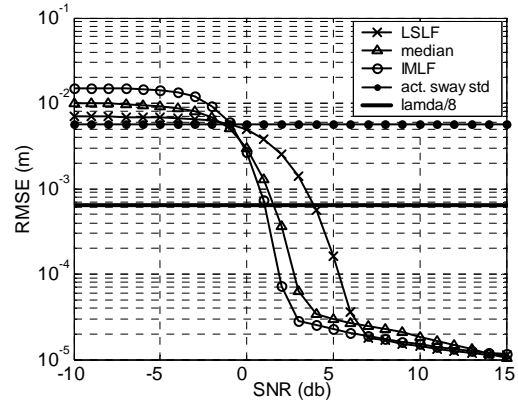


Fig. 4. Comparison of sway estimation method by sway estimation error (RMSE) (m) vs. SNR. The cross curve is using LSLF sway estimation method, the triangle curve is using median sway estimation method and the circle curve is using IMLF method. Each point is the root mean square error of sway estimation. The error is the estimated sway to the active sway. The RMSE is calculated for SNR from -10db to 15db. The point line is the standard deviation of the active sway distribution, and is independent of SNR. The black line shows the position of $\lambda/8$, λ is the wave length of the ping signal.

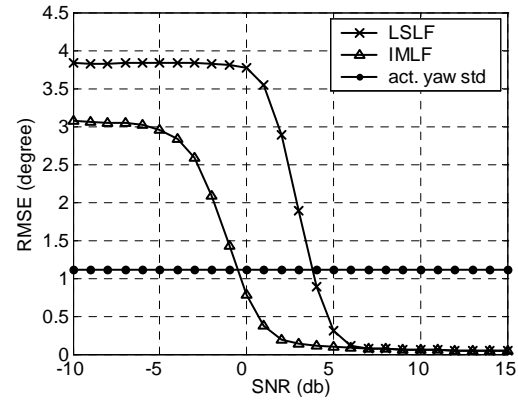


Fig. 5. Comparison of yaw estimation error (RMSE) (degree) vs. SNR. The cross curve is using LSLF method. The triangle curve is using IMLF method. Each point is the root mean square error of yaw estimation. The error is between the estimated yaw and the actual yaw. The RMSE is calculated for SNR form -10db to 15db. The point line is the standard deviation of the active yaw degrees distribution, it is independent of SNR.

and LSLF is 6db. Meanwhile, the RMSE of IMLF is over the std of the active yaw at -1db, but the LSLF is at 3db. From Fig. 4 and 5, it follows that the IMLF estimator is more robust than LSLF estimator for the estimation of sway or the estimation of yaw.

The next simulation aimed at demonstrating the improvement of sonar accuracy resulting by the improved motion estimation. 50 pings were transmitted and the received signals were contaminated by noise for each receive sensor and corrupted by motion for each ping. The time delay of the target was estimated from single ping and the temporal

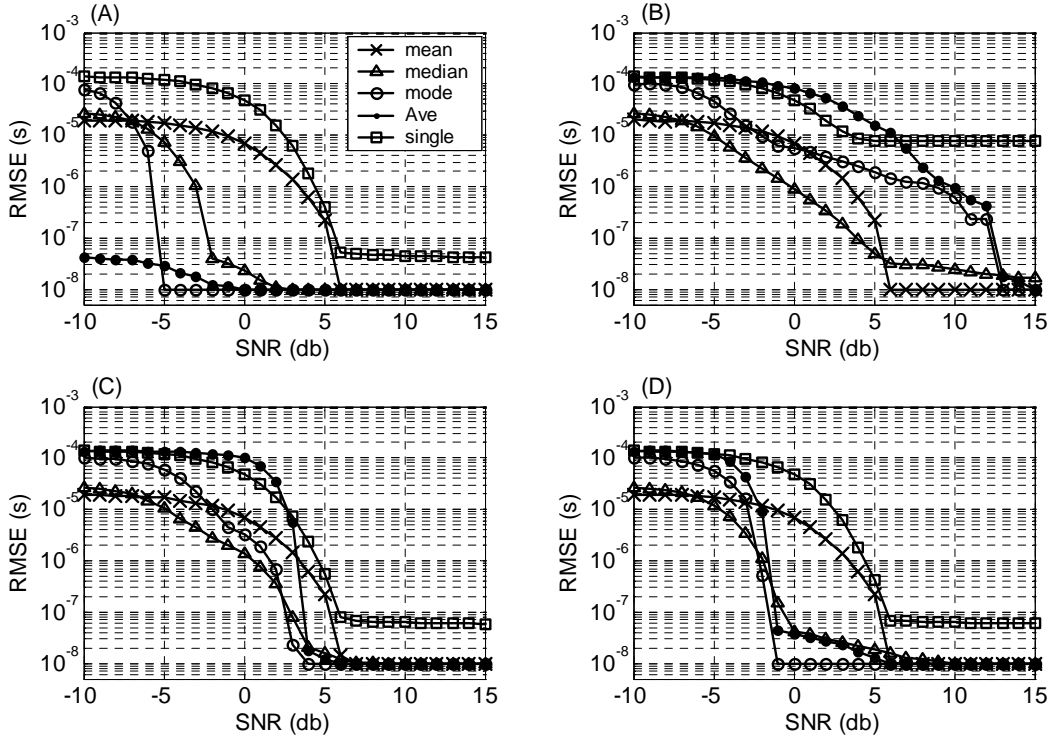


Fig. 6. Comparison of the motion corruption and the improvement after motion estimation for time delay estimation accuracy. Plot (A) is the ideal case where there is no motion between pings. Plot (B) is the worst case where the motion between pings is not corrected. Plot (C) is a moderate case where LSLF motion estimation is used to correct the motion between pings. Plot (D) is the best case where IMLF motion estimation is used to correct the motion. In each plot, time-delay estimation error (RMSE) (s) as a function of SNR is shown for different time-delay estimation methods. Each point is the root mean square error of time-delay estimation. The RMSE is calculated for SNR from -10db to 15db . The square curve is the estimation from a single ping. The cross curve, triangle curve and circle curve are the estimation based on the temporal mean, median and mode of multiple pings' estimation respectively. The point curve is the result of using the analog average of multiple pings to estimate the time delay.

mean, median and mode of multiple pings' estimation were calculated. The time delay of the analog average (Ave) of multiple pings is also estimated. The process is repeated by 200 times and the RMSE of the time delay estimation as a function of SNR is computed for each time delay estimation method. Fig. 6 depicts the Woodward curve of the delay estimation error (RMSE) (s) as a function of SNR and delay estimation method. Plot (A) shows the ideal case where there is no motion between pings. As one can predict, the analog average of multiple pings gives the best time delay estimation due to the reduction of noise. The mode function achieves more robust estimation than the median or the mean of the multiple pings. Plot (B) shows the worst case where time delay is estimated based on uncorrected motion pings. Although the average of multiple pings reduces the effect of noise, at the same time the signal also averaged because there is no signal overlay between pings due to the motion. In this case, the mode function and the median function produce better estimation. Plot (C) is the moderate result after using LSLF estimation to correct the sway and yaw. As we can see, the breakpoint of mode function and average function are

reduced to 4db . This attributes to the fact that the LSLF motion estimator can correct the motion between pings above noise SNR of 4db (see Fig. 4 and 5). Plot (D) shows the sonar accuracy after using IMLF estimation to correct the motion. The IMLF motion estimation makes an evident improvement of the time delay estimation accuracy. Using the mode function of multiple pings' estimation, the breakpoint is decreased to -1db which is close to the ideal case result. The RMSE of IMLF is smaller than that of LSLF when the SNR is above the breakpoint for any time delay estimation method (mean, median, mode and average). This verifies that IMLF gives better motion correction than LSLF. It demonstrates that IMLF method can estimate the motion correctly even when very strong noise is present. Subsequently both the accuracy and the resilience to noise are improved by the fusion of multiple pings after realignment according to the motion estimation.

IV. CONCLUSION

In this paper, a motion estimation scheme using multi-sensor signal based on improved mode line fitting algorithm (IMLF) was developed. The sway and yaw between two pings can be estimated simultaneously. We demonstrated that a robust algorithm based on multi-sensor, such as IMLF, significantly decreases the signal-to-noise ratio breakpoint for motion estimation. Taking advantage of the motion estimation, multiple pings after realignment are useful for improving the accuracy and the resilience of time-delay estimation to background noise. The performance of IMLF and LSLF algorithm was compared. The simulation results showed nearly perfect motion estimation using IMLF at SNR higher than 3db. Even lower to -1db noisy environment, accurate motion estimation can be obtained for partial pings using IMLF algorithm. That is enough to improve the accuracy of time-delay estimation by using multiple pings fusion. The simulation result shows that the fusion of multiple pings after realignment has the potential of improving both the resilience to noise and the accuracy, consequently increasing the sonar's operating range.

REFERENCE

- [1] R. J. McAulay and L. P. Seidman, "A useful form of the Barankin lower bound and its application to PPM threshold analysis," *IEEE Trans. Inform. Theory*, vol. IT-15, pp. 273-279, 1969.
- [2] J. M. Silkaitis, B. L. Douglas, and H. Lee, "A cascade algorithm for estimating and compensating motion error for synthetic aperture sonar imaging," in *IEEE Proc. ICIP*, vol. 1, pp. 905-909, Nov. 1994.
- [3] G. A. Shippey, P. Ulriksen, and Q. Liu, "Quasi-barrowband processing of wideband sonar echoes," in *Proc. 4th ECUA*, Rome, Italy, 1998, pp. 63-68.
- [4] K. A. Johnson, M. P. Hayes, and P. T. Gough, "Estimating sub-wavelength sway of sonar towfish," *IEEE J. Ocean. Eng.*, vol. 20, no. 4, pp. 258-267, Oct. 1995.
- [5] H. J. Callow, "Signal processing for synthetic aperture sonar image enhancement," Ph.D. dissertation, Univ. of Canterbury, Christchurch, New Zealand, Apr. 2003.
- [6] A. Bellettini and M. A. Pinto, "Experimental investigation of synthetic aperture sonar micronavigation," in *Proc. 5th ECUA*, Lyon, France, 2000, pp. 445-450.
- [7] J. T. Christoff, "Motion-compensated high frequency synthetic aperture sonar," *J. Acoust. Soc. Amer.*, vol. 1, pp. 2950, 1998.
- [8] V. Tonard and M. Brussieux, "Towards development of autofocusing schemes for phase compensation of synthetic aperture sonars," in *Proc. Oceans Conf.*, Oct. 1997, vol. 2, pp. 803-808.
- [9] P. T. Gough and M. A. Miller, "Displaced ping imaging autofocus for a multi-hydrophone SAS," *IEE Proc. Radar Sonar Navig.*, vol. 151, no. 3, pp. 163-170, June 2004.
- [10] C. Yuan, M. R. Azimi-Sadjadi, J. Wilbur, and G. J. Dobeck, "Underwater target detection using multichannel subband adaptive filtering and high-order correlation schemes," *IEEE J. Ocean. Eng.*, vol. 25, no. 1, Jan. 2000.
- [11] N. Neretti, N. Intrator, and L. N. Cooper, "Pulse-train based time-delay estimation improves resiliency to noise," *IEEE International Workshop on Machine Learning for Signal Processing*, Brazil, Sep. 2004, pp.213-222.
- [12] J. A. Jensen, "User's guide for the Field II program, Version 2.72," Technical Report, Technical Univ. of Denmark, DK-2800 Lyngby, Denmark, May 1999.